

Third-order elastic constants of germanium between 300 and 3°K†

James A. Bains, Jr. and M. A. Breazeale

Department of Physics, The University of Tennessee, Knoxville, Tennessee 37916

(Received 3 November 1975)

The ultrasonic harmonic-generation technique has been improved to the point that both amplitude and phase of the second harmonic of an initially sinusoidal ultrasonic wave in a solid can be measured between room temperature and 3°K. By measuring along the principal crystallographic directions, we have been able to determine temperature dependence of linear combinations of third-order elastic (TOE) constants of germanium. Between room temperature and 77°K the magnitude of the TOE constants does not vary greatly as a function of temperature. Between 77 and 3°K, C_{111} changes by +3%, $(C_{112} + 4C_{166})$ changes by +16%, and $(6C_{144} + C_{123} + 8C_{456})$ changes by -150%. All of these combinations of TOE constants are negative at 77°K, but below 7°K the combination $(6C_{144} + C_{123} + 8C_{456})$ is positive. Temperature dependence of additional combinations is inferred by assuming that the "Anderson-Grüneisen parameter" is independent of temperature.

I. INTRODUCTION

The present work is an extension to very low temperatures of previously established techniques for measuring third-order elastic (TOE) constants. The technique involves the measurement of the distortion of an ultrasonic wave as it propagates through the solid. This distortion was observed in polycrystalline aluminum,¹ and in several single crystals² with quartz transducers. The measurement technique was refined with the development of a capacitive receiver.³ This refinement, and subsequent ones,⁴ allowed absolute amplitude measurements to be made at different temperatures. Such measurements have been used by a number of investigators⁵ to calculate combinations of truly adiabatic TOE constants. Yost and Breazeale⁶ combined results from using this technique with those of Dunham and Huntington⁷ to obtain the first complete set of truly adiabatic TOE constants (of fused silica) at room temperature. TOE constants of copper⁸ have been measured between room temperature and 80°K. More recently we reported⁹ data on germanium between room temperature and 80°K. (This publication⁹ is hereinafter referred to as I.) The present measurements were undertaken to extend the data on TOE constants on germanium to lower temperatures in an attempt to answer a fundamental question about the relationship between the elastic and the thermal properties.

The thermal expansion of germanium is anomalous below 80°K.¹⁰ A similar anomaly has been observed in all other diamond lattice materials measured to date.¹¹ At temperatures below approximately $0.2\theta_0$ where θ_0 is the Debye temperature at 0°K, the thermal expansion changes from positive to negative and then becomes positive again at even lower temperatures. Calculations of the thermal expansion from the second-

order elastic (SOE) constants and TOE constants^{12,13,14} have not predicted the measured anomalous behavior at low temperatures. However, these calculations were based on the assumption that the TOE constants are not dependent on temperature (in lieu of actual data of TOE constant behavior at low temperature). We chose germanium for these low-temperature measurements to examine the validity of this assumption.

II. EXPERIMENTAL TECHNIQUE

Pure mode propagation is possible for a longitudinal ultrasonic wave in the three principal directions of a cubic crystal. In these special directions, the wave equation takes on the following form¹⁵:

$$\rho_0 \ddot{u} = K_2 \frac{\partial^2 u}{\partial a^2} + (3K_2 + K_3) \frac{\partial u}{\partial a} \frac{\partial^2 u}{\partial a^2} \quad (1)$$

where K_2 and K_3 are combinations of SOE and TOE constants, respectively, given in Table I.

If there is an initially sinusoidal disturbance at $a = 0$, this equation has the solution

$$u = A_1 \sin(ka - \omega t) - [(3K_2 + K_3)/8K_2] \times A_1^2 k^2 a \cos 2(ka - \omega t), \quad (2)$$

where k is the propagation constant $2\pi/\lambda$, a is the

TABLE I. K_2 and K_3 for principal directions of a cubic crystal.

Direction	K_2	K_3
[100]	C_{11}	C_{111}
[110]	$\frac{1}{2}(C_{11} + C_{12} + 2C_{44})$	$\frac{1}{4}(C_{111} + 3C_{112} + 12C_{166})$
[111]	$\frac{1}{3}(C_{11} + 2C_{12} + 4C_{44})$	$\frac{1}{3}(C_{111} + 6C_{112} + 12C_{144} + 24C_{166} + 2C_{123} + 16C_{456})$

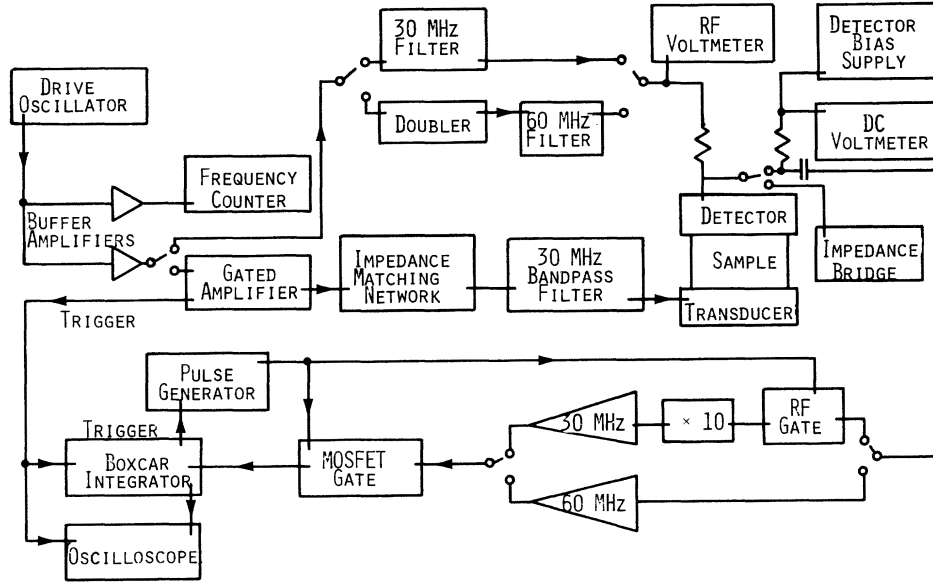


FIG. 1. Block diagram for room-temperature measurements.

propagation distance in the sample, and A_1 is the amplitude of the fundamental.

Thus the initially sinusoidal wave becomes distorted: a second harmonic is generated and grows linearly with propagation distance in the sample. The amplitude A_2 of this second harmonic is given by

$$A_2 = -[(3K_2 + K_3)/8K_2] A_1^2 k^2 a. \quad (3)$$

This harmonic distortion is the basis of the non-linearity measurements in the present work. The parameter K_3 may be calculated by

$$K_3 = -3K_2(\beta + 1), \quad (4)$$

where

$$\beta \equiv \frac{8}{3} (A_2/A_1^2) (1/k^2 a), \quad (5)$$

and the parameter K_2 may be found from the relation

$$K_2 = \rho_0 v^2, \quad (6)$$

where v is the velocity of sound in the appropriate direction in the medium.

A. Room-temperature measurements

A block diagram of the apparatus for making room-temperature measurements is shown in Fig. 1. A radio-frequency pulse of approximately 30 MHz is applied to an x-cut quartz transducer which is bonded to one end of the sample. The ultrasonic wave which propagates through the sample is detected at the other end by a capacitive receiver. In addition, provision is made to place a substitutional signal on the capacitive receiver so that accurate amplitude measurements can be made.

The air-gap capacitive receiver used is essentially the same as that described in detail by Gauster and Breazeale.³ A 1.016-cm diam electrode is placed approximately 5 μm from the sample (both surfaces being optically flat), and a dc bias on the order of 150 V is applied across the gap through a large resistor (approximately 1 M Ω).

The method of introducing the substitutional signal differs somewhat from that previously used by Peters, Breazeale, and Pare⁸ and in I. Previously the capacitive receiver itself had been removed from the circuit during the calibration procedures, and the calibrating signal was introduced through a substitutional capacitor, so that the equivalent circuit of the capacitive receiver (an ideal voltage generator in series with the capacitance of the receiver) was replaced by a real generator (whose voltage can be measured with a voltmeter) in series with the substitutional capacitor. (A second substitutional capacitor corrected for stray capacitance from the receiver to ground.)

In the present measurements, no circuit elements were substituted during the calibration. A substitutional signal which gave the same output as the ultrasonic signal was introduced across the capacitive receiver in such a way that the current of the substitutional signal could be measured. This current i can be related to the amplitude A of the ultrasonic wave by

$$i = 2AV_b \omega c/s, \quad (7)$$

where V_b is the dc bias on the receiver, ω is the angular frequency, c is the capacitance of the receiver, and s is the spacing of the capacitive re-

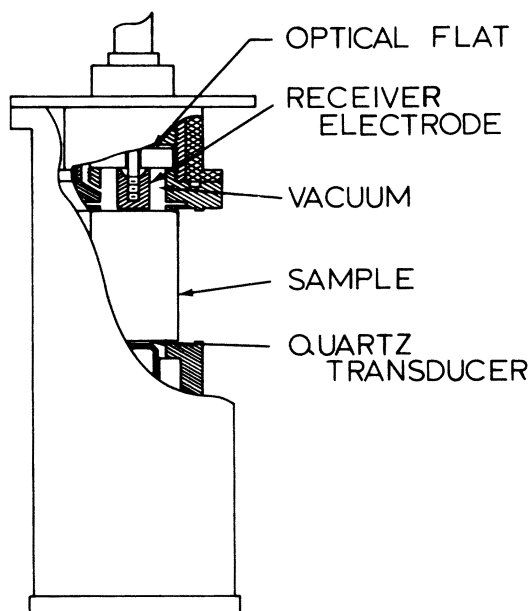


FIG. 2. Cutaway view of cryogenic apparatus.

ceiver plates.

The signal from the capacitive receiver is taken to either a 30- or 60-MHz bandpass amplifier. This amplified signal is detected and taken to a boxcar integrator. The boxcar integrator selects a portion of the first echo and gives a signal out which is proportional to the time average of that portion of the echo. The germanium samples, being nonconductors, do not sufficiently shield the rf pulse at the transducer from the receiver, so that a 30 MHz pulse is received at the receiver (by radiation) before the ultrasonic wave reaches the receiver. This "feedthrough" pulse can be much larger than the echo of interest and, although it can be separated in time from the measured echo, it can overload the 30 MHz amplifier and the boxcar integrator. This problem was solved by gating the signal from the capacitive receiver so that only the echo of interest was passed.

After the fundamental and second-harmonic signals have been measured by the boxcar integrator, the continuous wave (cw) substitutional signal is introduced at the capacitive receiver. The 60 MHz substitutional signal is derived by doubling the 30 MHz signal with a ring bridge mixer. Both the 30 and 60 MHz substitutional signals are filtered to ensure spectral purity. These two signals are adjusted to give the same output from the boxcar integrator as the ultrasonic signals and are then measured with an rf voltmeter. From these measurements and a knowledge of the circuit impedances (which were obtained at each frequency used by measurements

with a vector voltmeter), the current of the substitutional signal can be calculated.

B. Second-order elastic constants

The SOE constants were determined from room-temperature velocity measurements and the results were compared with the data of McSkimin and Adreatch¹⁶ and McSkimin.¹⁷ The agreement was within experimental error. The extensive tabulated data of McSkimin¹⁷ were used in the calculations of the cryogenic data.

C. Cryogenic apparatus

The electronic apparatus for making measurements at low temperature is essentially the same as that for measuring at room temperature. Since relative measurements can be made, it is not necessary to calibrate at each temperature. Thus, a reference voltage is not necessary.

As shown in Fig. 2, the sample holder is enclosed in a stainless-steel can. This can shown is surrounded by another can. The space between the cans is evacuated to provide an insulating jacket around the inner can, and the cans are polished to reduce radiation losses. The cans are supported by three thin-walled cupro-nickel tubes. Two of the tubes have a smaller cupro-nickel tube centered inside to provide a 50- Ω coaxial transmission line and are also used as vacuum lines. The other tube houses the temperature sensor and heater leads, and also is used to supply a pressure to the inner can.

The capacitive receiver is similar to that in the room temperature apparatus, with the additional feature that the gap spacing can be controlled pneumatically.⁴ The lapped ring against which the sample rests is undercut to make it a flexible diaphragm approximately 0.038 cm thick. The space above the sample is evacuated and the capacitor gap spacing is adjusted by regulating the pressure in the inner can.

The entire apparatus is suspended inside a standard helium research dewar. The dewar can be sealed and temperatures below the room-pressure boiling point of the coolant may be obtained by pumping on the coolant (either liquid helium or nitrogen).

The temperature in the inner can is controlled by an electric resistance heater connected to a commercial temperature controller, and can be varied continuously from approximately 3°K to room temperature.

D. Cryogenic nonlinearity measurements

Only relative measurements need to be taken with the cryogenic apparatus. One firsts adjusts the driving signal to the quartz transducer so that

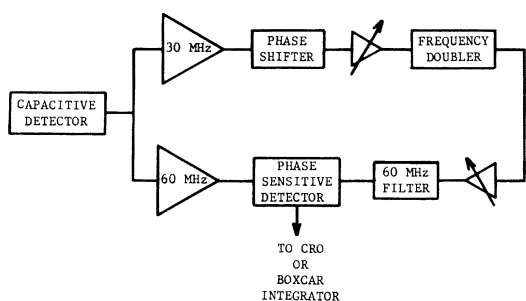


FIG. 3. Block diagram of phase-sensitive detector system.

the fundamental ultrasonic wave received at the capacitive receiver is the same at each temperature. The second harmonic is then measured by a slide-back technique: the dc bias voltage on the capacitive receiver is adjusted so that the electrical signal coming from the capacitive receiver is the same at all temperatures. The second-harmonic amplitude A_2 of the ultrasonic wave at two different temperatures (T_1 and T_2) are then related by

$$A_2(T_2) = A_2(T_1) V_b(T_1)/V_b(T_2). \quad (8)$$

The electrical feedthrough is worse in the cryogenic apparatus than it is in the room temperature apparatus. Therefore, a 60-MHz bandpass filter is used between the capacitive receiver and the amplifier to attenuate the 30-MHz feedthrough while passing the 60-MHz signal.

During the course of our measurements it became necessary to determine not only the magnitude of the second-harmonic amplitude, but also its sign. This resulted from the fact that K_3 were observed to change enough that they conceivably could have gone through zero. Such a condition would have been indicated by a phase shift of 180° in the second harmonic. For this reason we perfected a phase-sensitive detector to measure the sign of the second harmonic. (Phase-sensitive detectors which operate at 60 MHz are not commercially available to our knowledge.)

A block diagram of the phase sensitive detector system is shown in Fig. 3. A signal from the capacitive receiver is fed through a power splitter to a 30-MHz amplifier and a 60-MHz amplifier. The output of the 30-MHz amplifier is fed through a continuously variable phase shifter to a frequency doubler. This frequency doubled 30-MHz pulse echo train and the second-harmonic pulse echo train are fed into the phase-sensitive detector whose output is proportional to the cosine of the phase angle between the two 60-MHz signals. The phase shifter allows the phase angle between the two signals to be set to zero initially. If the sign of the second-harmonic amplitude changes

as the temperature is changed, the output of the phase-sensitive detector is inverted.

Using this phase sensitive detector system, we were able to make an unequivocal assignment of the phase to the second-harmonic amplitude used in the calculations of the linear combinations of TOE constants we call K_3 .

E. Samples

The samples used in this work, were the same ones used in I. These single crystals were 3.7803, 4.8242, and 3.4803 cm in the [100], [110], and [111] orientations, respectively. (The lengths are slightly changed since used in I because of lapping and recoating of the sample ends.) The sample ends were lapped and polished until optically flat and parallel to within 12 sec of arc. The ends were then made conductive by evaporating a copper coating approximation 1000 \AA thick onto them.

III. RESULTS

A. Room-temperature nonlinearity measurements for Ge

The absolute amplitude measurements at room temperature are given in Fig. 4. The straight lines in the figures are least-squares fits to the data points. It can be seen that the data will fit very well with a straight line; however, this line does not pass through the origin because of residual noise. The slope of the line is (in the least-squares sense) the best fit to the value of the quan-

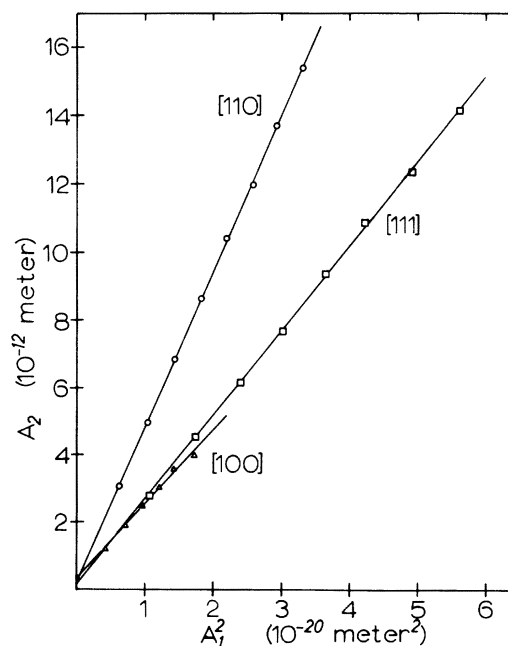


FIG. 4. Room-temperature values of the second-harmonic amplitude plotted as a function of the square of the fundamental amplitude.

TABLE II. Measured room-temperature values of β and K_3 .

Sample orientation	Sample Length (cm)	β				K_2^b (10^{11} dyn/cm 2)	K_3 (10^{12} dyn/cm 2)
		(Present value)	(Extrapolated from data of I) ^a	(average)			
[110]	4.8242	2.08 ± 0.015	1.977 (1.928)	2.029	15.51925	-14.10	
[111]	3.4803	1.71 ± 0.016	1.729 (1.633)	1.722	16.40807	-13.40	
[100]	3.7803	1.05 ± 0.044	0.989 (0.923)	1.018	12.85280	-7.782	

^aW. T. Yost and M. A. Breazeale, Phys. Rev. B **9**, 510 (1974).

^bFrom the data of H. J. McSkimin and P. Andreatch, Jr., J. Appl. Phys. **34**, 651 (1963).

tity

$$\frac{3}{8}\beta k_a^2 = k_a^2(3K_2 + K_3)/8K_2. \quad (9)$$

If the effect of the power lost from the fundamental to the second harmonic and by attenuation is considered, as was done in I, one finds that the present data satisfy the small amplitude assumption better than those in I. This can be seen in Fig. 5 in which we present values of the dimensionless parameter β calculated from both sets of data.

The data from I were corrected for the effect of residual noise in the equipment (which was not done previously). It is seen that the present data are best fit by a horizontal straight line and those of I are reasonably extrapolated in the manner described in that publication. The maximum difference between the sets of data is only 5.5%. In view of the fact that both measurements depend upon absolute measurements of displacement amplitudes on the order of 10^{-3} Å, this agreement is quite satisfying.

Further comparisons between the present results and the data of I are given in Table II. In the third column is the value of β obtained by a least-squares fit to the present data and its standard deviation. In the fourth column is the value of β extrapolated from the data of I, after correction for residual noise. For reference, values originally listed in I are given in parentheses in this column. In the fifth column the average between the two values of β are given, and this is taken as the most probable value. In the last column is given the value of K_3 calculated from the most probable value of β and the value of K_2 listed in column 6.

The random error for the present measurement is somewhat higher than that of I. This is in large part because the present measurements were made at much lower amplitudes. The systematic errors are estimated to be within plus or minus 10%. This estimate is consistent with the differences between the present work and data in I.

The values of β in the [110] and the [100] directions are approximately 5% and 5.5% higher than those of I, while the value of β in the [111] direction is approximately 0.8% lower than that of I. The present measurements of the [111] sample were made at 29.5 MHz, and the measurements of the [110] and the [100] sample were made at 30.0 MHz. The impedances in the room-temperature apparatus were measured at each frequency, and it is presumably errors associated with these impedance measurements which are mainly responsible for the differences between the present values of β and those of I.

B. Temperature dependence of TOE constants

Figure 6 shows the data we obtained for the three different K_3 's of germanium as a function

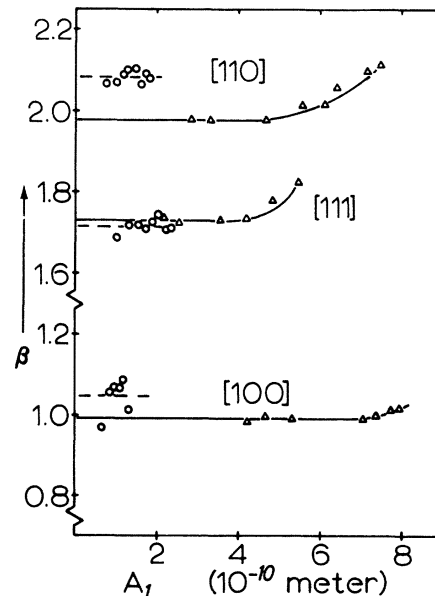


FIG. 5. Dimensionless parameter β plotted as a function of the fundamental amplitude. \circ present data; Δ data from I [W. T. Yost and M. A. Breazeale, Phys. Rev. B **9**, 510 (1974)].

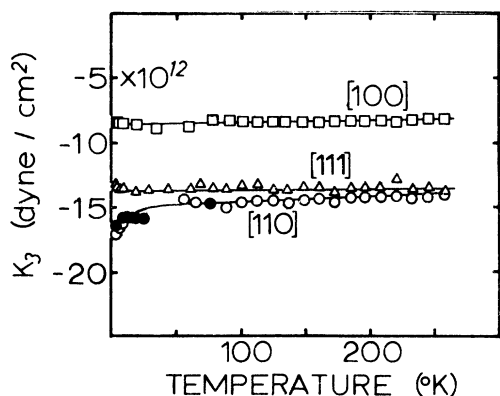


FIG. 6. Temperature dependence of the combinations of TOE constants K_3 for the three principal directions in Germanium.

of temperature. The first data runs, shown by the open symbols were taken without use of the phase-sensitive detector. The curves for the [100] and [111] directions are considered to be too smooth to admit a negative phase of the second harmonic from which the data were calculated. The data in the [110] direction were not

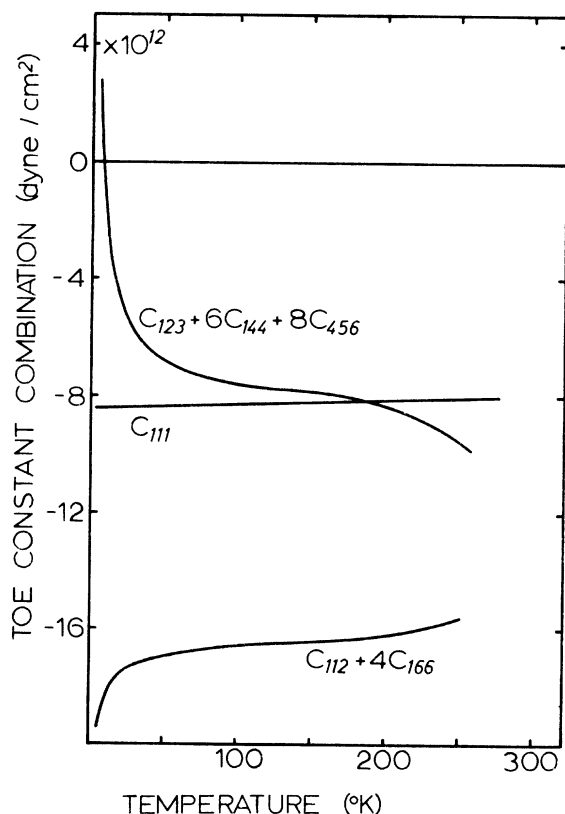


FIG. 7. Temperature dependence of the simplest combinations of TOE constants which can be calculated from the K_3 of Germanium.

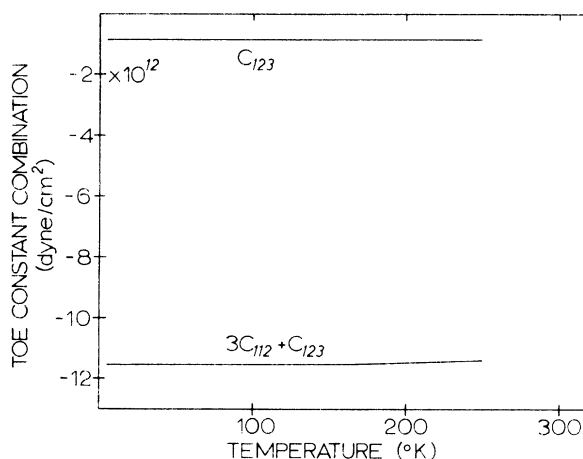


FIG. 8. Temperature dependence of certain TOE constants combinations calculated from our data under the assumption that the "Anderson-Grüneisen parameter" and C_{123} are temperature independent.

as smooth. The initial data between approximately 15 and 50° K had shown a peak or dip depending on the interpretation of the phase. We also noted that a thermal gradient might have been responsible for this behavior. The apparatus was modified to eliminate thermal gradients and the phase-sensitive detector was added. The data shown as solid circles were taken with the modified apparatus. There is no ambiguity about the sign of the second-harmonic amplitude from which these data were calculated. The agreement between the two sets of data in the low-temperature range reassured us about the correctness of these data and allowed us to eliminate erroneous data points from this plot.

Down to liquid-nitrogen temperature, these data reproduce the results of I to well within 3%. The data for the [100] direction can be fit very well with a straight line down to 3° K. The data for the [111] direction is essentially a straight line with a very slight upturn at very low temperatures. The data for the [110] direction are the only ones which show a marked deviation from a straight line. At low temperatures there is a definite downturn of the data.

These linear combinations of the TOE constants are not the simplest possible combinations available from our data. For example, C_{111} is contained in each of these curves, and therefore can be subtracted out. Proceeding in this fashion, we have evaluated the simplest combinations of TOE constants shown in Fig. 7.

As can be seen, there is not a great variation of these combinations of third-order elastic constants down to 77° K. But between 77 and 3° K there is a considerable variation in some of them. In particular, the combination ($C_{123} + 6C_{144} + 8C_{456}$)

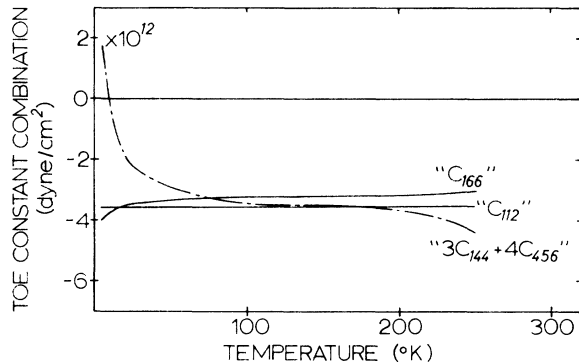


FIG. 9. Temperature dependence of certain TOE constant combinations calculated from our data assuming that both the "Anderson-Grüneisen parameter" and C_{123} are temperature independent.

crosses zero at 7 °K and becomes positive below that temperature. Since these are the TOE constants which would play a significant role in the transverse modes, we feel that the lack of agreement between theoretical calculation of thermal expansion from elastic data^{12,13,14} and the measured thermal expansion might be attributed to the theoretical assumption that the TOE constants are independent of temperature.

III. ISOLATION OF ADDITIONAL TOE CONSTANTS

Further reduction of the data can be made if one makes the assumption that the "Anderson-Grüneisen parameter"¹⁸ is not a function of temperature.¹⁹ This assumption may be more valid than the assumption that the TOE constants are independent of temperature. Therefore, using it to isolate additional TOE constants from our data may prove to be instructive.

Using the data from our experiment, the data

of McSkimin and Andreatch¹⁶ (combination of TOE constants at room temperature), and the data of McSkimin¹⁷ for the second-order constants C_{11} and C_{12} we can calculate the "Anderson-Grüneisen" parameter by Rao's formulation²⁰:

$$\delta = -1 - (C_{111} + 6C_{112} + 2C_{123}) / 3(C_{11} + 2C_{12}). \quad (10)$$

If δ is indeed constant as a function of temperature, then the temperature dependence of the combination $3C_{112} + C_{123}$ can be obtained from our data. Under this assumption, this combination of TOE constants shows virtually no temperature dependence (see Fig. 8). If it is further assumed that C_{123} is not a function of temperature (and equal to the room temperature value obtained from the data of our experiment and McSkimin and Andreatch), additional TOE constants may be calculated. These calculated constants are given in Fig. 9 and are designated by enclosing the constants in quotation marks to specify that these calculations are based on the two assumptions given above.

In conclusion, the measurements indicate that there is a definite temperature dependence of some of the TOE constants. Since we cannot isolate all of the TOE constants, it is not feasible at present to determine the effect of this temperature dependence on the Grüneisen parameter calculation of Brugger and Fritz.¹⁴ However, our assumption that the Anderson-Grüneisen parameter is independent of temperature has allowed us to plot most of the TOE constants as a function of temperature. The validity of this assumption, and hence of the curves drawn to Figs. 8 and 9, is open to question; however, one can observe that, to the extent these curves are valid, the greatest temperature dependence seems to be found in C_{166} and $3C_{144} + 4C_{456}$.

[†]Research supported in part by the U. S. Office of Naval Research. This paper is based in part on James A. Bains, Jr., doctoral dissertation, Dept. of Physics, The University of Tennessee, Knoxville, Tenn. 1974 (unpublished).

¹M. A. Breazeale and D. O. Thompson, *Appl. Phys. Lett.* **3**, 77 (1963).

²A. A. Gedroits and V. A. Krasilnikov, *Zh. Eksp. Teor. Fiz.* **43**, 1592 (1962) [*Sov. Phys.-JETP* **16**, 1122 (1963)].

³W. B. Gauster and M. A. Breazeale, *Rev. Sci. Instrum.* **37**, 1544 (1966).

⁴R. D. Peters, M. A. Breazeale, and V. K. Paré, *Rev. Sci. Instrum.* **39**, 1505 (1968).

⁵J. T. Mackey and R. T. Arnold, *J. Appl. Phys.* **40**, 4806 (1969); A. L. Sanford and S. P. Zehner, *Phys. Rev.* **153**, 1025 (1967); E. L. Meeks and R. T. Arnold, *Phys. Rev. B* **1**, 982 (1970).

⁶W. T. Yost and M. A. Breazeale, *J. Appl. Phys.* **44**,

1909 (1973).

⁷R. W. Dunham and H. B. Huntington, *Phys. Rev. B* **2**, 1098 (1970).

⁸R. D. Peters, M. A. Breazeale, and V. K. Paré, *Phys. Rev. B* **1**, 3245 (1970).

⁹W. T. Yost and M. A. Breazeale, *Phys. Rev. B* **9**, 510 (1974).

¹⁰S. I. Novikova, *Fiz. Tverd. Tela*, **2**, 43 (1960) [*Sov. Phys.-Solid State* **2**, 37 (1960)]; R. D. McCammon and G. K. White, *Phys. Rev. Lett.* **10**, 234 (1963).

¹¹P. W. Sparks and C. A. Swenson, *Phys. Rev.* **163**, 779 (1967); H. E. V. Erfling, *Ann. Phys. (Leipz.)* **41**, 467 (1942); D. F. Gibbons, *Phys. Rev.* **112**, 136 (1958).

¹²J. G. Collins, *Philos. Mag.* **8**, 323 (1963).

¹³D. E. Schuele and C. S. Smith, *J. Phys. Chem. Solids* **25**, 801 (1964).

¹⁴K. Brugger and T. C. Fritz, *Phys. Rev.* **157**, 524

- (1967).
- ¹⁵M. A. Breazeale and J. Ford, *J. Appl. Phys.* 36, 3486 (1965).
- ¹⁶H. J. McSkimin and P. Andreatch, Jr., *J. Appl. Phys.* 34, 651 (1963).
- ¹⁷H. J. McSkimin, *J. Appl. Phys.* 24, 988 (1953).
- ¹⁸O. L. Anderson, *Phys. Rev.* 144, 553 (1966).
- ¹⁹Y. A. Chang, *J. Phys. Chem. Solids* 28, 697 (1967).
- ²⁰R. R. Rao, *Phys. Rev. B* 10, 4173 (1974).